Non-Fermi liquid in a truncated two-dimensional Fermi surface

A. Ferraz*
Center for Theoretical Studies–Theoretische Physik, ETH-Hongerberg, CH-8093 Zurich
and Institut de Physique Theorique, Universite de Fribourg, Perolles, Chemin du Musee 3, CH-1700 Fribourg, Switzerland

(Received 20 December 2002; revised manuscript received 12 May 2003; published 26 August 2003)

Using perturbation theory and the field theoretical renormalization group approach we consider a two-dimensional anisotropic truncated Fermi Surface (FS) with both flat and curved sectors which approximately simulates the ''cold'' and ''hot'' spots in the cuprate superconductors. We calculate the one-particle two-loop irreducible functions $\Gamma^{(2)}$ and $\Gamma^{(4)}$ as well as the spin, the charge and pairing response functions up to one-loop order. We find nontrivial infrared stable fixed points and we show that there are important effects produced by the mixing of the existing scattering channels in higher order of perturbation theory. Our results indicate that the ''cold'' spots are turned into a non-Fermi liquid with divergents $\partial\Sigma_0/\partial p_0$ and $\partial\Sigma_0/\partial\overline{p}$, a vanishing Z, and either a finite or zero ''Fermi velocity'' at the FS when the effects produced by the flat portions are taken into account.

DOI: 10.1103/PhysRevB.68.075115 PACS number(s): 71.27.+a, 71.10.Hf, 74.20.Mn

I. INTRODUCTION

The appearance of high-T_c superconductivity focused everyone's attention on the properties of strongly interacting two-dimensional electron systems. Basically the high-T_c cuprates are characterized by a doping parameter which regulates the amount of charge concentration in the CuO_2 planes. As one varies the doping concentration and temperature one finds an antiferromagnetic phase, a pseudo-gap phase, an anomalous metallic phase and a d-wave superconductor.

The standard model to describe these phenomena is the two-dimensional $(2d)$ Hubbard model. Starting either from the so-called weak coupling limit or from the large U limit instead one can reproduce at least in qualitative terms all those phases by varying only a small number of appropriate parameters.[1] In particular, for the underdoped and optimally doped compounds, motivated by the experimental results coming from angle-resolved photoemission (ARPES) experiments which demonstrated among other things the presence of an anisotropic electronic spectra characterized by a pseudogap and flat bands in **k** space several workers have related some of these anomalies to the existence of a nonconventional Fermi surface (FS) in these materials.[2] As is well known for the half-filled $2d$-Hubbard model the FS being perfectly square the perfect nesting and the presence of van Hove singular points allow the mapping of this system onto perpendicular sets of one-dimensional chains[3] producing infrared divergences in both particle-particle and particle-hole channels, already at one-loop level. The physical system in this case shows a non-Fermi-liquid behavior. However, as doping is increased the FS immediately acquires curved sectors and this opens up a possibility for Fermi-liquid-like behavior around certain regions of **k** space. This feature seemed to be confirmed early on by the ARPES data for the underdoped and optimally doped Bi2212 and YBCO compounds.[4] In the electronic spectra of these materials there appears an anisotropic pseudogap and flat bands around $(\pm\pi,0)$ and $(0,\pm\pi)$ and traces of gapless single-particle band dispersions around the $(\pm\pi/2,\pm\pi/2)$ regions of the Brillouin zone (BZ). This agrees qualitatively well with the phenomenological picture of a FS composed of ''hot'' and ''cold'' spots put forwarded by Hlubina and Rice and Pines and co-workers.[5] In that picture the ''cold'' spots associated with correlated quasiparticle states are located along the BZ diagonals. In contrast the ''hot'' spots centered around $(\pm\pi,0)$ and $(0,\pm\pi)$ are related to the pseudogap and other anomalies of the cuprate normal phase. However, recent photoemission experiments[6] which have a much better resolution than before put into doubt the applicability of Fermi liquid theory even along the (0,0)- (π,π) direction. Using their data on momentum widths as a function of temperature for different points of FS, in optimally doped Bi2212, Valla *et al.* show that the imaginary part of the self-energy $\mathrm{Im}\,\Sigma$ scales linearly with the binding energy along that direction independent of the temperature. Similarly, Kaminski *et al.* show that the half-width-half-maximum of the spectral function $A(\mathbf{p},\omega)$ single particle peak varies linearly with ω above T_c. They claim this to be analogous to both the observed linear temperature behavior of the electrical resistivity and the scattering rate. Those results are very different from what is expected from a Fermi liquid and support a marginal Fermi-liquid phenomenology even near the $(\pi/2,\pi/2)$ points of the Brillouin zone.

In this work we consider a two-dimensional electron gas with a truncated FS composed of four symmetric patches with both flat and conventionally curve arcs in **k** space. These patches for simplicity are located around $(\pm k_F,0)$ and $(0,\pm k_F)$ respectively (Fig. 1). The Fermi-liquid-like states are defined around the patch center. In contrast the border regions are taken to be flat. As a result in this region the electron dispersion law is one dimensional.[7] In this way in each patch there are conventional two-dimensional electronic states sandwiched by single-particles with a flat FS to simulate the ''cold'' and ''hot'' spots scenario described earlier on. Flat FS sectors and single-particle with linear dispersion were also used earlier on by Dzyaloshinskii and co-workers[8] to produce logarithmic singularities and non-Fermi-liquid behavior. In their model the quasiparticle propagators depend explicitly only on the momenta perpendicular to the Fermi

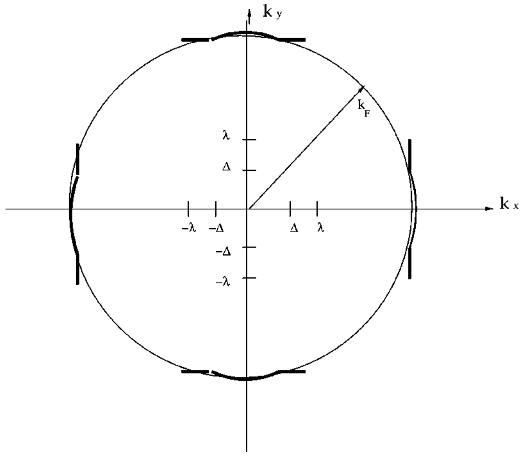

FIG. 1. Truncated Fermi surface model.

surface. The longitudinal momenta called by them ''fast variables'' are used to guarantee momentum conservation at every scattering process. By means of a symmetrization of those variables they distinguish between *s*- and *d*-wave superconductivities.

Here the flat sectors are mainly used to test the stability of the two-dimensional Fermi-liquid states associated with the ''curved'' parts of FS. We use the field theory renormalization group (RG) method to regularize the infrared (IR) singularities produced by the ''Cooper,'' ''exchange,'' and ''forward'' loops at every order of perturbation theory. These singular loops depend on the value of the external momenta as well as on the spin arrangements of the legs directly associated with them. Since these diagrams diverge at the Fermi surface the vertices acquire an explicit dependence on the values of the momenta along the FS in a way similar to what is done in the parquet type approach. However, in addition to considering two-loop order corrections we take explicit account of self-energy effects. This allows us to obtain nontrivial fixed points which are used to solve the RG equation for the single-particle propagator near the Fermi surface. We then use this result to calculate the momentum distribution function $n(\overline{p})$ and distinguish between those parts of the FS which remain metallic from the ones which are not.

Other RG methods were used recently by several workers to test the weak-coupling limit of the two-dimensional Hubbard model with and without next-nearest-neighbor hopping against superconducting and magnetic ordering as well as Pomenranchuk instabilities at different doping regimes.[9] However due to the difficulty in implementing their method in higher orders they do not go beyond one-loop and no self-energy effects are taken into account by them. As a result the coupling functions always have divergent flows and there is never any sign of the presence of nontrivial fixed points.

The scope of this work is the following. We begin by reviewing briefly the model used in our calculations. Next we calculate the one-particle irreducible functions $\Gamma^{(2)}_{\uparrow}$ and $\Gamma^{(4)}_{\uparrow\downarrow;\uparrow\downarrow}$ up to two-loop order. Our regularization scheme is introduced and discussed in detail. Using this procedure we demonstrate that the quasiparticle weight Z for the two-dimensional Fermi liquid state can vanish identically as a result of the interaction of the ''cold'' particles with the flat sectors. We solve the RG equation for the renormalized coupling in two-loop order and we find a nontrivial stable fixed point. From there we go on to solve the corresponding RG equation for the renormalized $\Gamma^{(2)}_{\uparrow}$ and to calculate the renormalized spectral function $A(\mathbf{p},\omega)$ when the physical system acquires its critical condition. Using $A(\mathbf{p},\omega)$ we calculate the momentum distribution function $n(\overline{p})$ and discuss the nature of the Fermi surface region associated the chosen fixed point value. Depending on the analytical properties of $\partial n(\overline{p})/\partial\overline{p}$ we can distinguish a metallic from an insulating-like behavior at the corresponding sector of the renormalized FS. Later, going beyond two-loops we estimate higher-order corrections. We take full account of the mixing of the various scattering channels and show how it affects our two-loop result. We conclude by emphasizing that our results indicate the instability of two-dimensional Fermi-liquid states when they are renormalized by the interaction with the flat sectors of the Fermi surface and by arguing that the resulting non-Fermi-liquid state may well be used to describe qualitatively the pseudogap phase of the cuprate superconductors.

II. TWO-DIMENSIONAL MODEL FERMI SURFACE

Consider a $2d$ FS consisting of four disconnected patches centred around $(\pm k_F,0)$ and $(0,\pm k_F)$. Let us assume to begin with that they are Fermi-liquid-like. The disconnected arcs separate occupied and unoccupied single-particle states along the direction perpendicular to the Fermi surface. However as we approach any patch along the arc itself there is no sharp resolution of states in the vicinity of the gaps located in the border regions. We assume that these regions are proper for non-Fermi-liquid (NFL) behavior. To represent those NFL features we take the FS to be flat in the border regions. In this way the single-particle states which are a $2d$ Fermi liquid around the center of the patch acquire an one-dimensional dispersion as we approach those flat border sectors. They represent the ''hot'' spots sandwiching the ''cold'' spots in our model.

In order to be more quantitative consider the single-particle Lagrangian density

$$\mathcal{L}=\sum_{\sigma}\ \psi^{\dagger}_{\sigma}(x)\left(i\partial_{\overline{t}}+\frac{\nabla^2}{2}+\overline{\varepsilon}_F\right)\psi_{\sigma}(x) -\overline{U}\psi^{\dagger}_{\uparrow}(x)\psi^{\dagger}_{\downarrow}(x)\psi_{\downarrow}(x)\psi_{\uparrow}(x), \tag{1}$$

where $x=(\overline{t},\mathbf{x})$, $\overline{\varepsilon}_F=k_F^2/2$, $\overline{t}^{-1}=m^*t^{-1}$, and $\overline{U}=m^*U$ with m^* being the effective mass. The Fermi surface parameters are now k_F, λ, and Δ. When we proceed with our renormalization scheme in the vicinity of a given FS point we replace k_F by the corresponding bare $k_F^0=Z^{-1}\omega^{1/2}\overline{k}_F$ where Z is the quasiparticle weight, $\overline{k}_F$ is dimensionless and ω is an energy scale parameter. In this way $\overline{k}_F$ can be nonzero even if both Z and $\omega\to 0$. The other Fermi surface parameters λ and Δ suffers the same kind of renormalization. Naturally the renormalization of the FS is in general much more intricate than this. Here we follow this route for simplicity. We can do this as long as we restrict the renormalization of those parameters to two-loop order and neglect the contribution of the constant Hartree term. In practice this is done simply by concentrating our attention in the most divergent contribution of the self-energy Σ as we show later on. We leave the discussion of the full implementation of a more general FS renormalization to a later work. Notice that in our scheme the coupling constant $\overline{U}$ scales as $\omega^{1-d/2}$ in d spatial dimensions. Here the fermion fields are nonzero only in a slab of width 2λ around the four symmetric patches of FS. Thus in momentum space the single-particle $\varepsilon(\mathbf{p})$ is defined according to the sector and FS patch under consideration. For example, in the vicinity of the central zone of the patch defined around the FS point $(0,-k_F)$, since there is a nonzero curvature in the FS we have that

$$\varepsilon(\mathbf{p})\cong\frac{k_F^2}{2}-k_F(p_y+k_F)+\frac{p_x^2}{2}, \tag{2}$$

with $-\Delta\leqslant p_x\leqslant\Delta$. In contrast in the border regions of the same patch where the FS is flat we find instead

$$\varepsilon(\mathbf{p})\cong\frac{k_F^2}{2}-k_F\left(p_y+k_F-\frac{\Delta^2}{2k_F}\right), \tag{3}$$

for $\Delta\leqslant p_x\leqslant\lambda$ or $-\lambda\leqslant p_x\leqslant-\Delta$. In this case only the single-particle dispersion depends exclusively on the momentum component perpendicular to the FS. We follow the same scheme to define $\varepsilon(\mathbf{p})$ in all other patches of the FS.

In setting up our perturbation theory scheme two quantities appear frequently: the particle-hole and the particle-particle bubble diagrams. In zeroth order they are defined, respectively, as

$$\chi^{(0)}_{\uparrow\downarrow}(P)=-\int_q G^{(0)}_{\uparrow}(q)G^{(0)}_{\downarrow}(q+P) \tag{4}$$

and

$$\Pi^{(0)}_{\uparrow\downarrow}(P)=\int_q G^{(0)}_{\uparrow}(q)G^{(0)}_{\downarrow}(-q+P), \tag{5}$$

where

$$G^{(0)}_{\uparrow}(q_0,\mathbf{q})=\frac{\theta[\overline{\varepsilon}(\mathbf{q})]}{q_0-\overline{\varepsilon}(\mathbf{q})+i\delta}+\frac{\theta[-\overline{\varepsilon}(\mathbf{q})]}{q_0-\overline{\varepsilon}(\mathbf{q})-i\delta} \tag{6}$$

with $\overline{\varepsilon}(\mathbf{q})=\varepsilon(\mathbf{q})-k_F^2/2$, $\int_q=-i\int(dq_0/2\pi)\int[d\mathbf{q}/(2\pi)^2]$, and $q=(q_0,\mathbf{q})$.

It turns out that $\chi^{(0)}$ is singular only if the $G^{(o)}$'s refer to flat sectors in which $\mathbf{q}$ and $\mathbf{q}+\mathbf{P}$ are points from corresponding antipodal border regions of the FS. In the case, in which e.g., $\mathbf{P}=(0,2k_F-\Delta^2/k_F)$ we find

$$\chi^{(0)}_{\uparrow\downarrow}(\mathbf{P};P_0)=\frac{(\lambda-\Delta)}{4\pi^2k_F}\left[\ln\left(\frac{\Omega+P_0-i\delta}{P_0-i\delta}\right)+\ln\left(\frac{\Omega-P_0-i\delta}{-P_0-i\delta}\right)\right] \tag{7}$$

with $\Omega=2k_F\lambda$.

In contrast $\Pi^{(0)}$ is singular for particles located in both "cold" and "hot" spots whenever they are involved in a Cooper scattering channel. Here for, e.g., $\mathbf{P}=(0,0)$ we obtain

$$\Pi^{(0)}_{\uparrow\downarrow}(\mathbf{P};P_0)=\frac{\lambda}{\pi^2k_F}\left[\ln\left(\frac{\Omega+P_0-i\delta}{P_0-i\delta}\right)+\ln\left(\frac{\Omega-P_0-i\delta}{-P_0-i\delta}\right)\right]. \tag{8}$$

As is well known the Cooper channel singularity drives the system towards its superconducting instability. However at one-loop for a repulsive interaction the renormalized coupling in that channel approaches the trivial Fermi liquid fixed point instead.[10] As opposed to that the singularity in $\chi^{(0)}$ produced by the one-loop exchange channel drives the physical system towards a nonperturbative regime. This nonperturbative behavior might be indicative of either the failure of the one-loop truncation or the inadequacy of perturbation theory itself to deal with that situation. To find out what is in fact the case we consider the effect of higher-order contributions in both one-particle irreducible functions $\Gamma^{(2)}(p)$ and $\Gamma^{(4)}(p)$.

III. ONE-PARTICLE IRREDUCIBLE FUNCTIONS

Let us initially consider the one-particle irreducible function $\Gamma^{(2)}_{\uparrow}(p_0,\mathbf{p})$ for a $\mathbf{p}$ located in the vicinity of a "cold" spot point of FS such as $\mathbf{p}^*=(\Delta,-k_F+\Delta^2/2k_F)$. We can write $\Gamma^{(2)}$ in this case as

$$\Gamma^{(2)}_{\uparrow}(p_0,\mathbf{p})=p_0+k_F\left(p_y+k_F-\frac{\Delta^2}{k_F}\right)-\Sigma_{\uparrow}(p_0,\mathbf{p}), \tag{9}$$

where, using perturbation theory, the two-loop self-energy $\Sigma_{\uparrow}$ is given by

$$\Sigma_{\uparrow}(p_0,\mathbf{p})=\frac{2U\lambda^2}{\pi^2}-2U^2\int_q G^{(0)}_{\downarrow}(q)\chi^{(0)}_{\uparrow\downarrow}(q-p). \tag{10}$$

The constant term produces at this order a constant shift in k_F which leads to the renormalization of the Fermi surface parameters λ and Δ. Since the renormalization of the Fermi surface is a problem in itself we postpone the discussion of its full implementation to a later work. Here for simplicity we ignore the presence of the constant term and concentrate our attention in the two-loop diagram which produces a non-analiticity at FS. As a result the renormalized Fermi surface parameters λ and Δ relate to their bare counterparts in the same way as k_F: $\lambda=Z\lambda_0$ and $\Delta=Z\Delta_0$.

Evaluating the integrals over q we obtain[11]

$$\Sigma_\uparrow(p_0,\mathbf{p})\cong -\frac{3U^2}{64\pi^4}\left(\frac{\lambda-\Delta}{k_F}\right)^2\left[p_0+k_F\left(p_y+k_F-\frac{\Delta^2}{2k_F}\right)\right]\times\left[\ln\left(\frac{\Omega+p_0-i\delta}{-k_F\left(p_y+k_F-\frac{\Delta^2}{2k_F}\right)+p_0-i\delta}\right)+\ln\left(\frac{\Omega-p_0-i\delta}{-k_F\left(p_y+k_F-\frac{\Delta^2}{2k_F}\right)-p_0-i\delta}\right)\right]. \tag{11}$$

Clearly both $\partial\Sigma_\uparrow/\partial p_y$ and $\partial\Sigma_\uparrow/\partial p_0$ are divergent at the FS. In fact it gives the marginal Fermi-liquid result[12] for $p_y=-k_F+\Delta^2/2k_F$ and $p_0=\omega\to 0$ which nullifies the quasiparticle weight $Z^{-1}=1-\partial\,\mathrm{Re}\,\Sigma_\uparrow/\partial p_0|_{\mathbf{p}^*;\omega}$ at the Fermi surface.

We can also arrive at this result by means of the renormalization group (RG). For this we define the renormalized one-particle irreducible function $\Gamma^{(2)}_{R\uparrow}(p_0,\mathbf{p})$ such that at $p_0=\omega$, where ω is a small energy scale parameter, and $\mathbf{p}=\mathbf{p}^*$, at the same Fermi surface point as before, $\Gamma^{(2)}_{R\uparrow}(p_0=\omega,\mathbf{p}=\mathbf{p}^*)=\omega$. Using the RG theory, $\Gamma^{(2)}_{R\uparrow}$ is related to the corresponding bare function $\Gamma^{(2)}_{0\uparrow}$ by

$$\Gamma^{(2)}_{R\uparrow}(p;U;\omega)=Z(\mathbf{p}^*;\omega)\Gamma^{(2)}_{0\uparrow}(p;U_0), \tag{12}$$

where U_0 and U are the corresponding bare and renormalized coupling. Since at zeroth order $U_0=U$ it follows immediately from our prescription and from perturbative result that

$$Z(\mathbf{p}^*;\omega)=\frac{1}{1+\frac{3U^2}{32\pi^4}\left(\frac{\lambda-\Delta}{k_F}\right)^2\ln\left(\frac{\Omega}{\omega}\right)}. \tag{13}$$

Naturally, $Z=0$ if $\omega\to 0$. As we show later this result reflects itself in the anomalous dimension developed by the single-particle Green's function at the FS.

Let us next calculate the one-particle irreducible two-particle function $\Gamma^{(4)}_{\alpha,\beta}(p_1,p_2;p_3,p_4)$ for $\alpha,\beta=\uparrow,\downarrow$. This function depends on the spin arrangements of the external legs as well as on the scattering channel into consideration. Generically for antiparallel spins up to two-loop order we have that

$$\Gamma^{(4)}_{\uparrow\downarrow}(p_1,p_2;p_3,p_4)=-U+U^2\int_k G^{(0)}_\uparrow(k)G^{(0)}_\downarrow(k+p_4-p_1)+U^2\int_k G^{(0)}_\uparrow(k)G^{(0)}_\downarrow(-k+p_1+p_2)-U^3\int_k G^{(0)}_\downarrow(k)G^{(0)}_\downarrow(k+p_3-p_1)\int_q G^{(0)}_\uparrow(q)\times G^{(0)}_\uparrow(q+p_3-p_1)+\cdots. \tag{14}$$

In one-loop order the only divergent contributions come from the particle-hole loop and the particle-particle diagram with internal lines with opposite spins. This singular particle-hole diagram with propagators with opposite spins we call exchange loop. In contrast, the forward loop is the divergent particle-hole diagram with internal lines of the same spin. This kind of loop only contributes to $\Gamma^{(4)}_{\uparrow\downarrow}$ from two-loop order on. However, the forward loop is present in every order of the perturbative series for the one-particle irreducible $\Gamma^{(4)}_{\uparrow\uparrow}$:

$$\Gamma^{(4)}_{\uparrow\uparrow}(p_1,p_2;p_3,p_4)=-U^2\int_k G^{(0)}_\downarrow(k)G^{(0)}_\downarrow(k+p_3-p_1)+U^3\int_k G^{(0)}_\downarrow(k)G^{(0)}_\downarrow(k+p_3-p_1)\Pi^{(0)}_{\uparrow\downarrow}(k+p_2)-U^3\int_k G^{(0)}_\downarrow(k)G^{(0)}_\downarrow(k+p_3-p_1)\chi^{(0)}_{\uparrow\downarrow}(p_4-k)+\cdots. \tag{15}$$

The nature of the singularities which appear in the perturbative series for $\Gamma^{(4)}_{\alpha,\beta}$ depend on the specific choice of the external momenta. Due to this momenta space anisotropy different kinds of scattering channels produce divergences with different multiplicative factors along the patched Fermi surface. They reflect the role played by the momenta along the FS in our results. As we will see later this automatically obliges us to define momenta dependent bare coupling functions in our perturbation series expansions. Despite all that the existing divergences can be grouped together with respect to their scattering channel and vertex type. This opens the way to define a systematic local regularization procedure to guide our renormalization group prescriptions throughout our calculations. Here our vertex classification convention goes as follows. We say there is an "exchange" type vertex whenever its associated "external" momenta can be tunned together to produce a logarithmic divergent exchange loop at the Fermi surface. This can be easily achieved if we choose to work in the " exchange" scattering channel for $\Gamma^{(4)}_{\uparrow\downarrow}$ in which the external momenta $\uparrow\mathbf{p}_1=\uparrow\mathbf{p}_3$ and $\downarrow\mathbf{p}_2=\downarrow\mathbf{p}_4$. In contrast if the external legs of $\Gamma^{(4)}_{\uparrow\downarrow}$ are chosen such that $\uparrow\mathbf{p}_1=\downarrow\mathbf{p}_4$ and $\downarrow\mathbf{p}_2=\uparrow\mathbf{p}_3$ it is now the "forward" particle-hole loop which becomes logarithmic divergent. The associated vertex in that case is then called "forward." Finally if the external legs of $\Gamma^{(4)}_{\uparrow\downarrow}$ are such that $\uparrow\mathbf{p}_1=-\mathbf{p}_2\downarrow$ and $\uparrow\mathbf{p}_3=-\downarrow\mathbf{p}_4$ the particle-particle diagram becomes logarithmic divergent. The vertex associated with that singular particle-particle diagram is said to be "Cooper-like."

In this work for simplicity we consider only the leading divergence at every order of perturbation theory. Despite that since we go beyond one-loop order and since we include nontrivial self-energy corrections we take explicitly into account contributions which are not considered either in parquet type or numerical RG approaches. Inasmuch as both the renormalization conditions and the bare coupling functions vary as we move along in momenta space, strictly speaking, we would need an infinite number of counterterms to regularize all the divergences in our model. However since all the divergences are associated with a singular loop with vertices which are either of exchange, Cooper or forward type it is possible to define three bare coupling functions $U_{0x}(\mathbf{p}_4-\mathbf{p}_1)$, $U_{0C}(\mathbf{p}_1+\mathbf{p}_2)$, and $U_{0f}(\mathbf{p}_3-\mathbf{p}_1)$ which cancel out exactly, order by order, all the divergences which appear in our perturbation theory expansions.

To illustrate our argument further take initially, e.g., $\mathbf{p}_1=\mathbf{p}_3=(\Delta,k_F-\Delta^2/2k_F)$ and $\mathbf{p}_2=\mathbf{p}_4=(\lambda-\epsilon,-k_F+\Delta^2/2k_F)$ with ϵ being such that $0\leqslant\epsilon<\lambda-\Delta$. The leading terms up to two-loop order for $p_0\approx 0$ are [Fig. 2(a)]

$$\begin{aligned}
&\Gamma^{(4)}_{\uparrow\downarrow}(\mathbf{p}_1=\mathbf{p}_3;\mathbf{p}_2=\mathbf{p}_4,p_0)\\
&\quad=-U-U^2\chi^{(0)}_{\uparrow\downarrow}(\mathbf{p}_4-\mathbf{p}_1;p_0)+U^2\Pi^{(0)}_{\uparrow\downarrow}(\mathbf{p}_1+\mathbf{p}_2;p_0)\\
&\qquad-U^3[\chi^{(0)}_{\uparrow\downarrow}(\mathbf{p}_4-\mathbf{p}_1;p_0)]^2-U^3[\Pi^{(0)}(\mathbf{p}_1+\mathbf{p}_2;p_0)]^2\\
&\qquad-U^3\int_k G^{(0)}_{\uparrow}(k)G^{(0)}_{\downarrow}(k+p_4-p_1)\Pi^{(0)}_{\uparrow\downarrow}(k+p_2)\\
&\qquad+U^3\int_k G^{(0)}_{\uparrow}(k)G^{(0)}_{\downarrow}(-k+p_1+p_2)\\
&\qquad\times[\chi^{(0)}_{\uparrow\downarrow}(p_4-k)+p_4\rightleftharpoons p_3]+\cdots.
\end{aligned}\tag{16}$$

If we evaluate all those diagrams we find

$$\begin{aligned}
&\Gamma^{(4)}_{\uparrow\downarrow}(\mathbf{p}_1=\mathbf{p}_3;\mathbf{p}_2=\mathbf{p}_4,p_0\approx\omega)\\
&\quad=-U-\frac{U^2}{2\pi^2k_F}\epsilon\ln\left(\frac{\Omega}{\omega}\right)+\frac{U^2}{2\pi^2k_F}(\lambda-\Delta-\epsilon)\ln\left(\frac{\Omega}{\omega}\right)\\
&\quad-\frac{U^3}{4\pi^4k_F^2}\epsilon^2\left[\ln\left(\frac{\Omega}{\omega}\right)\right]^2-\frac{U^3}{4\pi^4k_F^2}(\lambda-\Delta-\epsilon)^2\left[\ln\left(\frac{\Omega}{\omega}\right)\right]^2\\
&\quad+\frac{U^3}{16\pi^4k_F^2}\Bigg[3\epsilon\left(\lambda-\Delta-\frac{\epsilon}{2}\right)\\
&\quad+[(\lambda-\Delta)^2-\epsilon^2]\Bigg]\left[\ln\left(\frac{\Omega}{\omega}\right)\right]^2+\cdots.
\end{aligned}\tag{17}$$

In contrast for external momenta such as $\mathbf{p}_1=-\mathbf{p}_2=(\Delta,k_F-\Delta^2/2k_F)$ and $\mathbf{p}_3=-\mathbf{p}_4=(\lambda-\epsilon,-k_F+\Delta^2/2k_F)$ up to two-loop order our series expansion becomes instead [Fig. 2(b)]

$$\begin{aligned}
&\Gamma^{(4)}_{\uparrow\downarrow}(\mathbf{p}_1=-\mathbf{p}_2;p_0)\\
&\quad=-U+U^2\Pi^{(0)}_{\uparrow\downarrow}(p_0)-U^2\chi^{(0)}_{\uparrow\downarrow}(\mathbf{p}_4-\mathbf{p}_1;p_0)\\
&\qquad-U^3(\Pi^{(0)}_{\uparrow\downarrow}(p_0))^2-U^3[\chi^{(0)}_{\uparrow\downarrow}(\mathbf{p}_4-\mathbf{p}_1;p_0)]^2\\
&\qquad+U^3\int_k G^{(0)}_{\downarrow}(k)G^{(0)}_{\uparrow}(-k;p_0)[\chi^{(0)}_{\uparrow\downarrow}(p_3-k)\\
&\qquad+\chi^{(0)}_{\uparrow\downarrow}(p_4-k)]\\
&\qquad-U^3\int_k G^{(0)}_{\uparrow}(k)G^{(0)}_{\downarrow}(k+p_4-p_1)\Pi^{(0)}(k+p_2)+\cdots.
\end{aligned}\tag{18}$$

Evaluating those integrals we obtain

$$\begin{aligned}
&\Gamma^{(4)}_{\uparrow\downarrow}(\mathbf{p}_1=-\mathbf{p}_2;p_0)\\
&\quad=-U+\frac{U^2}{2\pi^2k_F}(4\lambda)\ln\left(\frac{\Omega}{\omega}\right)-\frac{U^2}{4\pi^2k_F}(\lambda-\Delta-\epsilon)\ln\left(\frac{\Omega}{\omega}\right)\\
&\qquad-\frac{U^3}{4\pi^4k_F^2}(4\lambda)^2\left[\ln\left(\frac{\Omega}{\omega}\right)\right]^2-\frac{U^3}{16\pi^4k_F^2}(\lambda-\Delta-\epsilon)^2\\
&\qquad\times\left[\ln\left(\frac{\Omega}{\omega}\right)\right]^2+\frac{U^3}{16\pi^4k_F^2}\left[\frac{3}{2}(\lambda-\Delta)^2+2\epsilon(\lambda-\Delta-\epsilon)\right]\\
&\qquad\times\left[\ln\left(\frac{\Omega}{\omega}\right)\right]^2+\frac{U^3}{16\pi^4k_F^2}[(\lambda-\Delta)^2-\epsilon^2]\left[\ln\left(\frac{\Omega}{\omega}\right)\right]^2\\
&\qquad+\cdots.
\end{aligned}\tag{19}$$

Finally, if we now choose external momenta such as $\mathbf{p}_1=\mathbf{p}_4=(\Delta,k_F-\Delta^2/2k_F)$ and $\mathbf{p}_2=\mathbf{p}_3=(\lambda-\epsilon,-k_F+\Delta^2/2k_F)$ we have that $\mathbf{p}_3-\mathbf{p}_1=(\lambda-\Delta-\epsilon,-2k_F+\Delta^2/k_F)$, $\mathbf{p}_1+\mathbf{p}_2=(\lambda+\Delta-\epsilon)$ and our series expansion in the forward channel becomes [Fig. 2(c)]

$$\begin{aligned}
&\Gamma^{(4)}_{\uparrow\downarrow}(\mathbf{p}_1=\mathbf{p}_4;\mathbf{p}_2=\mathbf{p}_3,p_0)\\
&\quad=-U+U^2\Pi^{(0)}(\mathbf{p}_1+\mathbf{p}_2;p_0)-U^3[\chi^{(0)}_{\uparrow\uparrow}(\mathbf{p}_3-\mathbf{p}_1;p_0)]\\
&\qquad\times[\chi^{(0)}_{\downarrow\downarrow}(\mathbf{p}_3-\mathbf{p}_1;p_0)]-U^3[\Pi^{(0)}(\mathbf{p}_1+\mathbf{p}_2;p_0)]^2\\
&\qquad+U^3\int_k G^{(0)}_{\uparrow}(k)G^{(0)}_{\downarrow}(-k+p_1+p_2)\\
&\qquad\times[\chi^{(0)}_{\uparrow\downarrow}(p_4-k)+p_4\rightleftharpoons p_3]\\
&\qquad+U^3\int_k G^{(0)}_{\downarrow}(k+p_3-p_1)G^{(0)}_{\uparrow}(k)\chi^{(0)}_{\uparrow\downarrow}(p_4-k)+\cdots.
\end{aligned}\tag{20}$$

Solving all those integrals above we get

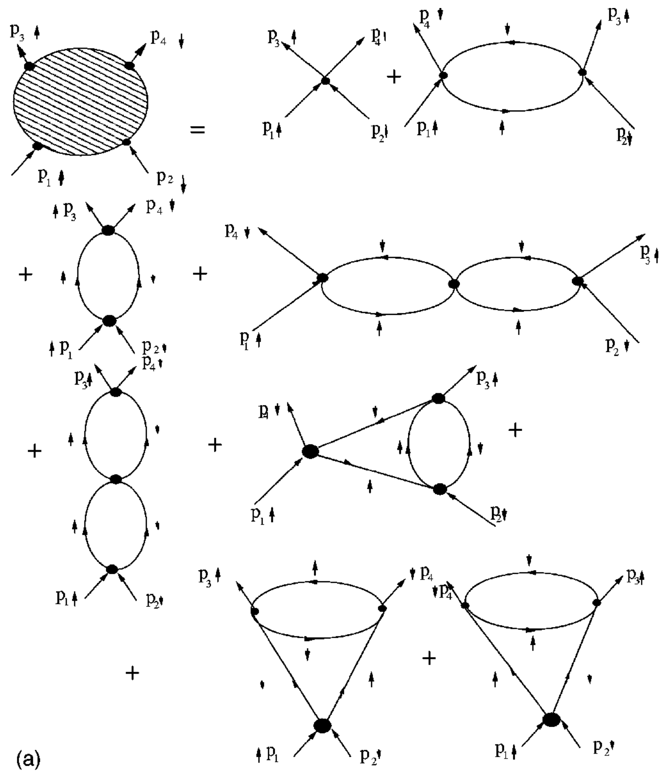

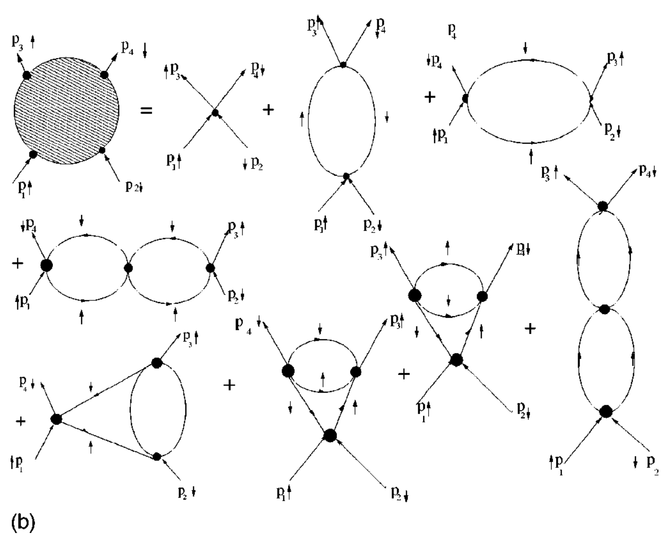

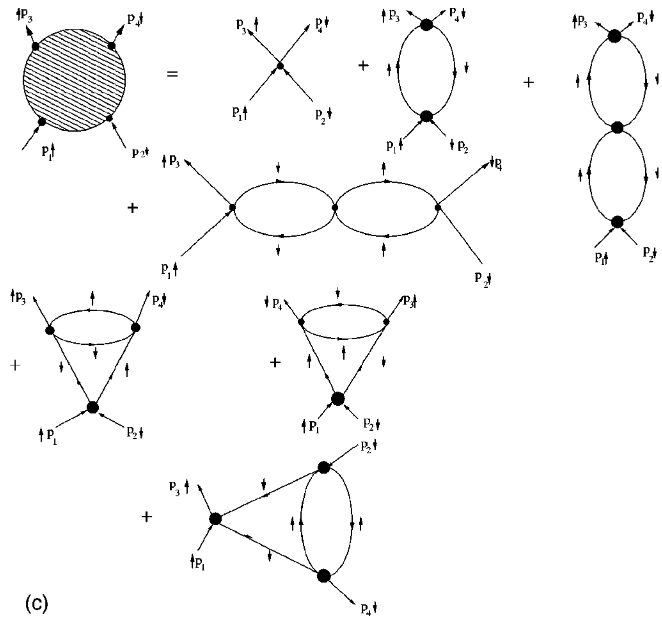

FIG. 2. Feynmann diagrams up to two-loop order for $\Gamma^{(4)}_{\uparrow\downarrow}$ in the (a) exchange channel, (b) Cooper channel, and (c) forward channel.

$$\Gamma^{(4)}_{\uparrow\downarrow}(\mathbf{p}_1=\mathbf{p}_4;\mathbf{p}_2=\mathbf{p}_3,p_0)$$
$$=-U+\frac{U^2}{2\pi^2 k_F}(\lambda-\Delta-\epsilon)\ln\left(\frac{\Omega}{\omega}\right)-\frac{U^3}{16\pi^4 k_F^2}(\epsilon)^2\times\left[\ln\left(\frac{\Omega}{\omega}\right)\right]-\frac{U^3}{16\pi^4 k_F^2}(\lambda-\Delta-\epsilon)^2\left[\ln\left(\frac{\Omega}{\omega}\right)\right]^2+\frac{U^3}{16\pi^4 k_F^2}[(\lambda-\Delta)^2-\epsilon^2]\left[\ln\left(\frac{\Omega}{\omega}\right)\right]^2+\cdots. \quad (21)$$

Our renormalization prescription must therefore incorporate this momenta space anisotropy to cancel all the corresponding singularities appropriately.

Using RG theory we can proceed with the regularization scheme relating the renormalized two-particle function $\Gamma^{(4)}_{R\uparrow\downarrow}$ to its corresponding bare function $\Gamma^{(4)}_{0\uparrow\downarrow}$

$$\Gamma^{(4)}_{R\uparrow\downarrow}[p_1,p_2;p_3,p_4;U_a(\{\mathbf{p}_i\};\omega);\omega]=\prod_{i=1}^{4} Z_i^{1/2}(\mathbf{p}_i;\omega)\Gamma^{(4)}_{0\uparrow\downarrow}[p_1,p_2;p_3,p_4;U_{0a}(\{\mathbf{p}_i\})], \quad (22)$$

where U_{0a} and U_a are the bare and the renormalized couplings respectively with $a=x$ (exchange), C (Cooper), f (forward). The renormalized $\Gamma^{(4)}_{R\uparrow\downarrow}$ can be invoked for the definition of the renormalized coupling functions. Here we follow a renormalization prescription regulated by the leading divergence in one-loop order. Thus if the leading divergence in one-loop order is the exchange particle-hole loop we define $\Gamma^{(4)}_{R\uparrow\downarrow}$ such that $\Gamma^{(4)}_{R\uparrow\downarrow}(\{\mathbf{p}_i\},p_0=\omega)=-U_x(\{\mathbf{p}_i\},\omega)$. In this way it follows that

$$\Gamma^{(4)}_{R\uparrow\downarrow}(\mathbf{p}_1=\mathbf{p}_3;\mathbf{p}_2=\mathbf{p}_4;p_0=\omega;U_a)=-U_x(\mathbf{p}_1=\mathbf{p}_3;\mathbf{p}_2=\mathbf{p}_4;\omega;U_a) \tag{23}$$

for $\mathbf{p}_1=\mathbf{p}_3=(\Delta,k_F-\Delta^2/2k_F)$ and $\mathbf{p}_2=\mathbf{p}_4=(\lambda-\epsilon,-k_F+\Delta^2/2k_F)$ with $2\epsilon>\lambda-\Delta$.

Similarly, if the leading divergence in one-loop order is the particle-particle Cooper diagram in our prescription the renormalized $\Gamma^{(4)}_{R\uparrow\downarrow}$ is such that $\Gamma^{(4)}_{R\uparrow\downarrow}(\{\mathbf{p}_i\};p_0=\omega;U_a)=-U_C(\{\mathbf{p}_i\};\omega;U_a)$. Clearly using this scheme

$$\Gamma^{(4)}_{R\uparrow\downarrow}(\mathbf{p}_1=-\mathbf{p}_2;p_0=\omega;U_a)=-U_C(\mathbf{p}_1=-\mathbf{p}_2;\omega;U_a) \tag{24}$$

for $\mathbf{p}_1=-\mathbf{p}_2=(\Delta,k_F-\Delta^2/2k_F)$ and $\mathbf{p}_3=-\mathbf{p}_4=(\lambda-\Delta-\epsilon,k_F-\Delta^2/2k_F)$.

Finally if the leading particle-hole loop has internal lines with the same spin $\Gamma^{(4)}_{R\uparrow\downarrow}$ in our prescription $\Gamma^{(4)}_{R\uparrow\downarrow}(\{\mathbf{p}_i\},p_0=\omega;U_a)=-U_f(\{\mathbf{p}_i\};\omega;U_a)$. It follows from this that

$$\Gamma^{(4)}_{R\uparrow\downarrow}(\mathbf{p}_1=\mathbf{p}_4;\mathbf{p}_2=\mathbf{p}_3,p_0=\omega;U_a)=-U_f(\mathbf{p}_1=\mathbf{p}_4;\mathbf{p}_2=\mathbf{p}_3;\omega;U_a) \tag{25}$$

for $\mathbf{p}_1=\mathbf{p}_4=(\Delta,k_F-\Delta^2/2k_F)$ and $\mathbf{p}_2=\mathbf{p}_3=(\lambda-\epsilon,-k_F+\Delta^2/2k_F)$, respectively.

Using this renormalization scheme we find, respectively,

$$\begin{aligned}U_x(\mathbf{p}_1=\mathbf{p}_3;\mathbf{p}_2=\mathbf{p}_4;\omega;U_a)&=Z(\mathbf{p}_1;\omega)Z(\mathbf{p}_4;\omega)\Bigg(U_{0x}\Bigg\{1+\frac{\epsilon}{2\pi^2k_F}U_{0x}\ln\left(\frac{\Omega}{\omega}\right)\\&+\frac{1}{4\pi^2k_F^2}\left[\epsilon^2U_{0x}^2-\frac{3}{4}\epsilon\left(\lambda-\Delta-\frac{\epsilon}{2}\right)U_{0C}^2\right]\\&\times\left[\ln\left(\frac{\Omega}{\omega}\right)\right]^2+\cdots\Bigg\}-\frac{\lambda-\Delta-\epsilon}{2\pi^2k_F}U_{0C}^2\ln\left(\frac{\Omega}{\omega}\right)\\&+\frac{U_{0C}}{4\pi^4k_F^2}\bigg[(\lambda-\Delta-\epsilon)^2U_{0C}^2\\&-\frac{1}{4}[(\lambda-\Delta)^2-\epsilon^2]U_{0x}^2\bigg]\left[\ln\left(\frac{\Omega}{\omega}\right)\right]^2+\cdots\Bigg)\end{aligned} \tag{26}$$

for the exchange channel,

$$\begin{aligned}U_C(\mathbf{p}_1=-\mathbf{p}_2;\mathbf{p}_3=-\mathbf{p}_4;\omega;U_a)&=Z(\mathbf{p}_1;\omega)Z(\mathbf{p}_4;\omega)\Bigg(U_{0C}\Bigg\{1-\frac{4\lambda}{2\pi^2k_F}U_{0C}\ln\left(\frac{\Omega}{\omega}\right)\\&+\frac{1}{4\pi^2k_F^2}\bigg[(4\lambda)^2U_{0C}^2-\frac{1}{4}\bigg(\frac{3}{2}(\lambda-\Delta)^2\\&+2\epsilon(\lambda-\Delta-\epsilon)\bigg)U_{0x}^2\bigg]\left[\ln\left(\frac{\Omega}{\omega}\right)\right]^2\\&+\cdots+\frac{\lambda-\Delta-\epsilon}{4\pi^2k_F}U_{0x}^2\ln\left(\frac{\Omega}{\omega}\right)+\frac{U_{0x}}{16\pi^4k_F^2}\\&\times\{(\lambda-\Delta-\epsilon)^2U_{0x}^2-[(\lambda-\Delta)^2-\epsilon^2]U_{0C}^2\}\\&\times\left[\ln\left(\frac{\Omega}{\omega}\right)\right]^2+\cdots\Bigg)\end{aligned} \tag{27}$$

for the Cooper channel and finally

$$\begin{aligned}U_f(\mathbf{p}_1=\mathbf{p}_4;\mathbf{p}_2=\mathbf{p}_3;\omega;U_a)&=Z(\mathbf{p}_1;\omega)Z(\mathbf{p}_3;\omega)\Bigg\{U_{0f}\bigg[1+\frac{\epsilon^2}{4\pi^4k_F^2}\\&\times U_{0f}^2\ln^2\left(\frac{\Omega}{\omega}\right)+\cdots\bigg]-\frac{\lambda-\Delta-\epsilon}{2\pi^2k_F}U_{0C}^2\ln\left(\frac{\Omega}{\omega}\right)\\&+\frac{U_{0C}}{4\pi^4k_F^2}\bigg((\lambda-\Delta-\epsilon)^2U_{0C}^2\\&-\frac{1}{4}[(\lambda-\Delta)^2-\epsilon^2]U_{0x}^2\bigg)\left[\ln\left(\frac{\Omega}{\omega}\right)\right]^2+\cdots\Bigg\}\end{aligned} \tag{28}$$

for the forward channel. Here $Z(\mathbf{p}_1;\omega)$ is given as before and

$$Z^{-1}(\mathbf{p}_3;\omega)=1+\frac{U_{0x}^2}{16\pi^4k_F^2}\left[\frac{3}{2}(\lambda-\Delta)^2+3\epsilon(\lambda-\Delta-\epsilon)\right]\ln\left(\frac{\Omega}{\omega}\right)+\cdots. \tag{29}$$

These results can be simplified further if we take into consideration that the divergencies are removed by local subtractions. Thus if we restrict ourselves to two-loop order we must have $U_{0C}^2\cong U_{0x}^2\cong U_{0f}^2\cong U_0^2$. Up to two-loop order there is in practice no mixing of channels in our perturbation theory. As a result the RG equations for the renormalized coupling functions simplify considerably and they reduce to

$$U_x = U_{0x} - (aU_{0x}^2 - 2bU_{0x}^3)\ln\left(\frac{\Omega}{\omega}\right) + \cdots, \tag{30}$$

where

$$a = \frac{2\epsilon - (\lambda - \Delta)}{2\pi^2 k_F}, \tag{31}$$

$$b = \frac{3}{32\pi^4 k_F^2}[(\lambda - \Delta)^2 + \epsilon(\lambda - \Delta - \epsilon)], \tag{32}$$

$$U_f = U_{0f} - (cU_{0f}^2 + 2bU_{0f}^3)\ln\left(\frac{\Omega}{\omega}\right) + \cdots \tag{33}$$

with $c = (\lambda - \Delta - \epsilon)/2\pi^2 k_F$,

$$U_C = U_{0C} - (dU_{0C}^2 + 2bU_{0C}^3)\ln\left(\frac{\Omega}{\omega}\right) + \cdots \tag{34}$$

with $d = [4\lambda - (\lambda - \Delta - \epsilon)/2]/2\pi^2 k_F$.

Using the RG conditions $\omega\partial U_{0x}/\partial\omega = \omega\partial U_{0f}/\partial\omega = \omega\partial U_{0C}/\partial\omega = 0$ the RG equations for U_x, U_f and U_C in two-loop order are simply

$$\beta(U_x) = \omega\frac{\partial U_x}{\partial\omega} = -aU_x^2 + 2bU_x^3 + \cdots, \tag{35}$$

$$\beta(U_f) = \omega\frac{\partial U_x}{\partial\omega} = cU_f^2 + 2bU_f^3 + \cdots, \tag{36}$$

and

$$\beta(U_c) = \omega\frac{\partial U_c}{\partial\omega} = dU_c^2 + 2bU_c^3 + \cdots. \tag{37}$$

Note that there are nontrivial fixed points $U_x^* = a/2b$, $U_c^* = -\{[4\lambda - (\lambda - \Delta - \epsilon)/2]/[2\epsilon - (\lambda - \Delta)]\}U_x^*$ and $U_f^* = -\{(\lambda - \Delta - \epsilon)/[2\epsilon - (\lambda - \Delta)]\}U_x^*$ for the exchange, Cooper and forward channels respectively which are infrared (IR) stable but they are by no means of small magnitude if the renormalized Fermi surface parameters continue to be such that $k_F \gg (\lambda - \Delta)$ and $\lambda \gg (\lambda - \Delta)$. The magnitude of U_x^* is regulated by the ratio of k_F and the size of the flat sector of the FS for $\epsilon \cong \lambda - \Delta$. In this case the larger the size of the flat sector with respect to k_F the smaller the magnitude of U_x^*. For U_C^* and U_f^* there are extra multiplicative factors which measures basically the ratio of FS longitudinal widths in **k** space available for the divergent particle-particle and particle-hole diagrams in the Cooper and forward channels respectively. In our perturbation theory scheme the expansion parameter is precisely a fraction of U_a(width)$/k_F$ and even a large value of the coupling constant such as some of the U^*'s above present no serious convergence difficulty to our perturbation series expansions.

We can use a similar RG approach for the renormalized two-particle irreducible function with parallel spins. Now we define the corresponding one-particle irreducible function as

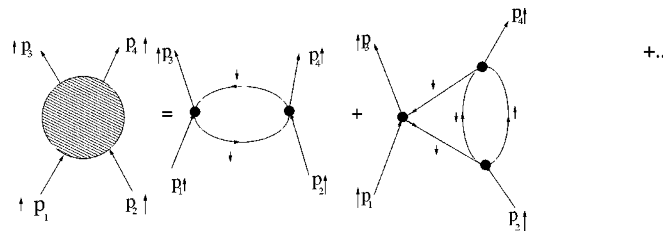

FIG. 3. Diagrams up two-loop order for $\Gamma^{(4)}_{\uparrow\uparrow}$.

$$\Gamma^{(4)}_{R\uparrow\uparrow}(p_1,p_2;p_3,p_4;U_a;\omega) = \prod_{i=1}^{4} Z_i^{1/2}(\mathbf{p}_i;\omega)\Gamma^{(4)}_{0\uparrow\uparrow}(p_1,p_2;p_3,p_4;U_{0a}) + A(\omega), \tag{38}$$

where $A(\omega)$ is an infinite additive constant which is defined to cancel the divergence produced by the first term in our perturbation series expansion for $\Gamma^{(4)}_{0\uparrow\uparrow}$. As a result of that our RG prescription in this case becomes $\Gamma^{(4)}_{R\uparrow\uparrow}(\{\mathbf{p}_i\};p_0 = \omega;U_a;\omega) = 0$. In this way it follows immediately that

$$\Gamma^{(4)}_{R\uparrow\uparrow}(\mathbf{p}_4 = \mathbf{p}_1;\mathbf{p}_2 = \mathbf{p}_3;p_0 = \omega;U_a;\omega) = Z(\mathbf{p}_1;\omega)Z(\mathbf{p}_3;\omega)[\Gamma^{(4)}_{0\uparrow\uparrow}(\mathbf{p}_4 = \mathbf{p}_1;\mathbf{p}_2 = \mathbf{p}_3; p_0 = \omega;U_{0a})] + A(\omega) = 0. \tag{39}$$

Using our perturbation series result (Fig. 3) we obtain

$$\Gamma^{(4)}_{0\uparrow\uparrow}(\mathbf{p}_1 = \mathbf{p}_4;\mathbf{p}_2 = \mathbf{p}_3,p_0 = \omega;U_{0a}) = \frac{\epsilon}{2\pi^2 k_F}U_{0f}^2\ln\left(\frac{\Omega}{\omega}\right) - \frac{U_{0f}U_{0C}^2}{16\pi^4 k_F^2} \times 3\epsilon\left(\lambda - \Delta - \frac{\epsilon}{2}\right)\ln^2\left(\frac{\Omega}{\omega}\right) + \cdots. \tag{40}$$

Using the same approximation $U_{0f}^2 \cong U_{0C}^2 \cong U_0^2$ as before it follows immediately that

$$A(\omega) = -\frac{\epsilon}{2\pi^2 k_F}U_f^2\ln\left(\frac{\Omega}{\omega}\right) + \frac{U_f^3}{16\pi^4 k_F^2}3\epsilon\left(\lambda - \Delta - \frac{\epsilon}{2}\right)\ln^2\left(\frac{\Omega}{\omega}\right) + \cdots. \tag{41}$$

Having established the existence of IR stable nontrivial fixed points in two-loop order we can now investigate how self-energy effects produce an anomalous dimension in the single-particle Green's function at the Fermi surface.[11]

IV. SINGLE-PARTICLE GREEN'S FUNCTION AND OCCUPATION NUMBER AT FS

We can use the RG to calculate the renormalized Green's function G_R at the FS. Since $G_R = (\Gamma_R^{(2)})^{-1}$ it follows from the previous section that

$$G_R(p_0;\mathbf{p}^*;\{U_a\};\omega)=Z^{-1}(\mathbf{p}^*;\omega)G_0(p_0;\mathbf{p}^*;\{U_{0a}\}), \tag{42}$$

where G_0 is the corresponding bare Green's function and $\mathbf{p}^*$ is some fixed FS point. Seeing that G_0 is independent of the scale parameter ω we obtain that G_R satisfies the Callan-Symanzik (CS) equation[13]

$$\left(\omega\frac{\partial}{\partial\omega}+\sum_a \beta_a(\{U_b\})\frac{\partial}{\partial U_a}+\gamma\right)G_R(p_0;\mathbf{p}^*;\{U_b\};\omega)=0, \tag{43}$$

where

$$\gamma=\omega\frac{d}{d\omega}\ln Z(\omega). \tag{44}$$

Using the fact that G_R at the FS is a homogeneous function of ω and p_0 of degree $D=-1$ it turns out that it must also satisfy the equation

$$\left(\omega\frac{\partial}{\partial\omega}+p_0\frac{\partial}{\partial p_0}\right)G_R(p_0;\mathbf{p}^*;\{U_a\};\omega)=-G_R(p_0;\mathbf{p}^*;\{U_a\};\omega). \tag{45}$$

Combining this with the CS equation we then find

$$\left(-p_0\frac{\partial}{\partial p_0}+\sum_a \beta_a(\{U_b\})\frac{\partial}{\partial U_a}+\gamma-1\right)\times G_R(p_0;\mathbf{p}^*;\{U_b\};\omega)=0. \tag{46}$$

Using the fact that up to two-loop order we don't yet distinguish the mixing effects produced by the different scattering channels in the self-energy we can simplify this RG equation even further. As a result we assume that the divergence up to this order is associated with just one of the renormalized coupling functions. If we choose U_x to be this coupling in consideration the CS equation reduces to

$$\left(-p_0\frac{\partial}{\partial p_0}+\beta_x(U_x)\frac{\partial}{\partial U_x}+\gamma-1\right)G_R(p_0;\mathbf{p}^*;U_x;\omega)=0. \tag{47}$$

From this we obtain that the formal solution for G_R is

$$G_R(p_0;\mathbf{p}^*;U_x;\omega)=\frac{1}{p_0}\exp\left(\int_\omega^{p_0}d\ln\left(\frac{\overline{p_0}}{\omega}\right)\gamma[U_x(\overline{p_0};\mathbf{p}^*;U_x)]\right), \tag{48}$$

where

$$\frac{dU_x(\overline{p_0};U)}{d\ln\left(\frac{\overline{p_0}}{\omega}\right)}=\beta_x[U_x(\overline{p_0};\mathbf{p}^*;U_x)], \tag{49}$$

with $U_x(\overline{p_0}=\omega;\mathbf{p}^*;U_x)=U_x(\mathbf{p}^*;\omega)$.

If we assume that as the physical system approaches the Fermi surface as $p_0\sim\omega\rightarrow 0$, it also acquires a critical condition with the running coupling constant $U_x(\mathbf{p}^*;\omega)\rightarrow U_x^*(\mathbf{p}^*)$ for $\mathbf{p}^*=(\lambda-\epsilon,-k_F+\Delta^2/2k_F)$ we can use our perturbation theory result for $Z(\mathbf{p}^*;\omega)$ up to order $O(U_x^{*2})$ to obtain

$$\gamma=\frac{3U_x^{*2}}{16\pi^4k_F^2}\left[\frac{(\lambda-\Delta)^2}{2}+\epsilon(\lambda-\Delta-\epsilon)\right]+\cdots=\gamma^*. \tag{50}$$

As a result G_R develops an anomalous dimension given by[11]

$$G_R(p_0;\mathbf{p}^*;U_x^*;\omega)=\frac{1}{\omega}\left(\frac{\omega^2}{p_0^2}\right)^{(1-\gamma^*)/2}. \tag{51}$$

If we make the analytical continuation $p_0\rightarrow p_0+i\delta$, at the FS, G_R reduces for $p_0<0$ to

$$G_R(p_0;U^*;\omega)=-\frac{1}{\omega}\left(\frac{\omega^2}{p_0^2}\right)^{[(1-\gamma^*)/2]}\times[\cos(\pi\gamma^*)+i\sin(\pi\gamma^*)]. \tag{52}$$

Using this result the spectral function $A(k_F,p_0)=-\operatorname{Im}G_R$ becomes

$$A(k_F,p_0)=\theta(-p_0)\left|\frac{p_0}{\omega}\right|^{\gamma^*}\frac{\sin(\pi\gamma^*)}{|p_0|} \tag{53}$$

and the number density $n(k_F)$ reduces to

$$n(k_F)=\frac{1}{2}\frac{\sin(\pi\gamma^*)}{\pi\gamma^*}. \tag{54}$$

Notice that if $U_x^*\rightarrow 0$, $\gamma^*\rightarrow 0$ and as a result $n(k_F;U_x^*=0)=\frac{1}{2}$. Alternatively, if we replace our two-loop value for U_x^* we get

$$\gamma^*=\frac{4}{3}[2\epsilon-(\lambda-\Delta)]^2\frac{[(\lambda-\Delta)^2/2+\epsilon(\lambda-\Delta-\epsilon)]}{[(\lambda-\Delta)^2+\epsilon(\lambda-\Delta-\epsilon)]^2}. \tag{55}$$

If we now take $\epsilon=\frac{2}{3}(\lambda-\Delta)$ we find $\gamma^*\cong 0.07$,

$$\operatorname{Im}G_R(p_0;U^*;\omega)\cong-\left(\frac{\omega^2}{p_0^2}\right)^{-0.035}\frac{1}{|p_0|}, \tag{56}$$

and as a result $n(k_F;U_x^*)\cong 0.14$. This result shows that there is indeed no discontinuity at $n(k_F)$. Moreover there is only a small correction to the marginal Fermi liquid result for the "cold" spot point which suffers the direct effect of the flat sectors through Σ. The correction to the linear behavior of $\operatorname{Im}\Sigma$ is practically not observed experimentally. The power law behavior of G_R and the value of $n(k_F)$ independent of the sign of the coupling constant resembles the results obtained for a Luttinger liquid.[14] However, for the one-dimensional Luttinger liquid $\partial n(p)/\partial p|_{p=k_F}\rightarrow\infty$. In order to see if the occupation function shows the same behavior in our case we have to generalize our CS equation to explicitly include the momentum dependence for G_R in the vicinity of a given "cold" spot point.

V. GREEN'S FUNCTION AND MOMENTUM DISTRIBUTION FUNCTION NEAR A "COLD" SPOT POINT

Let us choose for simplicity the point $\mathbf{p}^* = (\Delta - v, -k_F + \Delta^2/2k_F - v\Delta/k_F)$ in the $(0,-k_F)$ patch of our FS model. Quite generically the relation between the renormalized and bare one-particle irreducible $\Gamma^{(2)}$'s holds for any momentum value. Thus taking into consideration our perturbative two-loop self-energy result together with the fact that at $p_0=0$ and in the vicinity of the FS point $(\Delta - v, -k_F + (\Delta^2/2k_F) - (v\Delta/k_F))$, it is natural to define a renormalized $(k_F)_R$ such that $\Gamma_R^{(2)}$ reduces to

$$\Gamma_R^{(2)}(p_0=0,\mathbf{p};\omega) = \overline{p} = \left[k_F\left(p_y + k_F - \frac{\Delta^2}{2k_F} + \frac{v\Delta}{k_F}\right)\right]_R = Z(\mathbf{p}^*,\omega) k_F\left(p_y + k_F - \frac{\Delta^2}{2k_F} + \frac{v\Delta}{k_F}\right). \tag{57}$$

In this way the renormalization of all the Fermi surface parameters is emulated by $\overline{p}$.

In the presence of a nonzero $\overline{p}$ the CS equation for G_R in the neighborhood of this "cold" spot point becomes

$$\left(\omega \frac{\partial}{\partial \omega} + \beta(U_x)\frac{\partial}{\partial U_x} + \gamma \overline{p}\frac{\partial}{\partial \overline{p}} + \gamma\right) G_R(p_0;\overline{p};U_x;\omega) = 0. \tag{58}$$

Since now we have

$$\left(\omega \frac{\partial}{\partial \omega} + p_0 \frac{\partial}{\partial p_0} + \overline{p}\frac{\partial}{\partial \overline{p}}\right) G_R(p_0;\overline{p};U_x;\omega) = -G_R(p_0;\overline{p};U_x;\omega), \tag{59}$$

it follows from this that G_R satisfies the RG equation

$$\left(p_0 \frac{\partial}{\partial p_0} + (1-\gamma)\overline{p}\frac{\partial}{\partial \overline{p}} - \beta(U_x)\frac{\partial}{\partial U_x} + 1 - \gamma\right) \times G_R(p_0;\overline{p};U_x;\omega) = 0. \tag{60}$$

We can therefore write G_R in the form

$$G_R(p_0;\overline{p};U_x;\omega) = \mathcal{G}[U_x(p_0;U_x);\overline{p}(p_0;\overline{p})] \times \exp - \left(\int_\omega^{p_0} d\ln\left(\frac{\overline{p}_0}{\omega}\right)\{1-\gamma[U_x(\overline{p}_0;\overline{p};U_x)]\}\right), \tag{61}$$

where

$$\overline{p}(p_0;U_x) = \overline{p}\exp\left(- \int_\omega^{p_0} d\ln\left(\frac{\overline{p}_0}{\omega}\right)\{1-\gamma[U_x(\overline{p}_0;\overline{p};U_x)]\}\right), \tag{62}$$

and the β function is determined perturbatively. If we assume as before that the physical system is brought to criticality as $\omega \to 0$ and $U_x(\omega) \to U_x^* \neq 0$ we can use our perturbation theory result for γ and these equations reduce to

$$G_R(p_0;\overline{p};U_x^*;\omega) = \frac{1}{p_0}\mathcal{G}[\overline{p}(p_0;U_x^*)]\left(\frac{p_0}{\omega}\right)^{\gamma^*}, \tag{63}$$

with

$$\overline{p}(p_0;U_x^*) = \overline{p}\left(\frac{p_0}{\omega}\right)^{(\gamma^*-1)}. \tag{64}$$

The function $\mathcal{G}$ is determined from perturbation theory. Recalling that at zeroth order, for $p_0 \simeq \omega$, we have that

$$G_R \cong \frac{1}{\omega + \overline{p}} + O(U_x^{*2}), \tag{65}$$

and it turns out that

$$\mathcal{G}[\overline{p}(p_0;U_x^*)] = \frac{\omega}{\omega + \overline{p}(p_0:U^*)} + \cdots. \tag{66}$$

Finally, combining all these results we get that in the vicinity of our "cold" spot point

$$G_R(p_0;\overline{p};U_x^*;\omega) = \frac{1}{p_0}\left(\frac{p_0^2}{\omega^2}\right)^{\gamma^*/2}\left[1 + \frac{\overline{p}}{p_0}\left(\frac{p_0^2}{\omega^2}\right)^{\gamma^*/2}\right]^{-1}. \tag{67}$$

If we now do again the analytic continuation $p_0 \to p_0 + i\delta$ we obtain the renormalized Green's function in the form

$$G_R(p_0;\overline{p};U_x^*) = \frac{\left(\frac{p_0^2}{\omega^2}\right)^{\gamma^*/2}}{\overline{p}\left(\frac{p_0^2}{\omega^2}\right)^{\gamma^*/2} - |p_0|\cos(\pi\gamma^*) + i|p_0|\sin(\pi\gamma^*)}, \tag{68}$$

for $p_0 < 0$ or

$$G_R(p_0;\overline{p};U_x^*) = \frac{\left(\frac{p_0^2}{\omega^2}\right)^{\gamma^*/2}}{\overline{p}\left(\frac{p_0^2}{\omega^2}\right)^{\frac{\gamma^*}{2}} + p_0 + i\delta}, \tag{69}$$

for $p_0 > 0$.

It follows from this that the imaginary part of the renormalized self-energy $\mathrm{Im}\,\Sigma_R$, for $p_0 < 0$, is given by-

$$\mathrm{Im}\,\Sigma_R(p_0;\overline{p};U_x^*;\omega) = -|p_0|\left(\frac{p_0^2}{\omega^2}\right)^{-\gamma^*/2}\sin(\pi\gamma^*) \tag{70}$$

or $\mathrm{Im}\,\Sigma_R(p_0;\overline{p};U_x^*;\omega)=0$ for $p_0>0$.

As a result of that the renormalized spectral function $A_R(\overline{p};\omega)$ becomes[11]

$$A_R(p_0,\overline{p};\omega) = \frac{|p_0|\left(\frac{p_0^2}{\omega^2}\right)^{-\gamma^*/2}\sin(\pi\gamma^*)}{\left(\overline{p}-|p_0|\left(\frac{\omega^2}{p_0^2}\right)^{\gamma^*/2}\cos(\pi\gamma^*)\right)^2 + p_0^2\left(\frac{\omega^2}{p_0^2}\right)^{\gamma^*}\sin^2(\pi\gamma^*)}, \tag{71}$$

for $p_0<0$ or simply

$$A_R(p_0,\overline{p};\omega) = \frac{\pi}{1-\gamma^*}\left(\frac{p_0}{\omega}\right)^{\gamma^*}\delta\left(p_0-\left(\frac{-\overline{p}}{\omega}\right)^{1/(1-\gamma^*)}\right), \tag{72}$$

for $p_0>0$.

We can immediately infer from this result that our renormalized Fermi Surface near the given ‘‘cold’’ spot point is now characterized by a dispersion law given by

$$p_0 = \overline{E}(\overline{p}) = -\left(\frac{\overline{p}\sec(\pi\gamma^*)}{\omega^{\gamma^*}}\right)^{1/(1-\gamma^*)}, \tag{73}$$

for $p_0<0$, $\overline{p}>0$, and $\cos(\pi\gamma^*)\neq 0$ or

$$p_0 = \overline{E}(\overline{p}) = \left(\frac{-\overline{p}}{\omega}\right)^{1/(1-\gamma^*)} \tag{74}$$

for $p_0>0$ and $\overline{p}<0$.

If we now define the ‘‘Fermi velocity’’ v_F as the derivative of $\overline{E}(\overline{p})$ with respect to the component of the momentum perpendicular to the Fermi surface in the vicinity of $\mathbf{p}^*$ we find

$$v_F = \frac{k_{FR}}{1-\gamma^*}[\sec(\pi\gamma^*)]^{1/(1-\gamma^*)}\left(\frac{\overline{p}}{\omega}\right)^{\gamma^*/(1-\gamma^*)}, \quad p_0<0, \quad \overline{p}>0, \tag{75}$$

$$v_F = \frac{k_{FR}}{1-\gamma^*}\left(\frac{-\overline{p}}{\omega}\right)^{\gamma^*/(1-\gamma^*)}, \quad p_0>0, \quad \overline{p}<0. \tag{76}$$

Clearly for $\gamma^*/(1-\gamma^*)>0$ and we have that $v_F\to 0$ if $|\overline{p}|/\omega\to 0$. However if $(\gamma^*/(1-\gamma^*)\ll 1$, v_F is nonzero and differs only weakly from its k_{FR} value.

Finally, using our spectral function result we can calculate the momentum distribution function $n(\overline{p})$ for $\overline{p}/\omega\sim 0$. Using $n(\overline{p})=\int_{-\omega}^{\omega}(dp_0/2\pi)A_R(p_0,\overline{p};\omega)$, we obtain

$$n(\overline{p}) = \frac{1/2}{1-\gamma^*}\left(\frac{-\overline{p}}{\omega}\right)^{\gamma^*/(1-\gamma^*)}\theta(-\overline{p})\,\theta(1-\gamma^*) + |\sin(\pi\gamma^*)|\int_0^1\frac{dy}{2\pi}\frac{y^{1-\gamma^*}}{\left[y^{1-\gamma^*}-\frac{\overline{p}}{\omega}\exp i(\pi\gamma^*)\right]\left[y^{1-\gamma^*}-\frac{\overline{p}}{\omega}\exp -i(\pi\gamma^*)\right]}. \tag{77}$$

Evaluating this last integral we get

$$n(\overline{p}) = \frac{1/2}{1-\gamma^*}\left(\frac{-\overline{p}}{\omega}\right)^{\gamma^*/(1-\gamma^*)}\theta(-\overline{p}) + \frac{|\sin(\pi\gamma^*)|}{2\pi\gamma^*}\left(1+\frac{\gamma^*}{2\gamma^*-1}\frac{\sin(2\pi\gamma^*)}{\sin(\pi\gamma^*)}\frac{|\overline{p}|}{\omega}+\cdots\right) - \frac{\theta(1-\gamma^*)}{2\pi}\Gamma\left(\frac{2-\gamma^*}{1-\gamma^*}\right)\Gamma\left(\frac{-1}{1-\gamma^*}\right)\left(\frac{|\overline{p}|}{\omega}\right)^{\gamma^*/(1-\gamma^*)}\left[\theta(\overline{p})\sin\left(\frac{3\pi}{1-\gamma^*}\right)-\theta(-\overline{p})\sin\left(\frac{2\pi}{1-\gamma^*}\right)\right] \tag{78}$$

for $|\overline{p}|/\omega \ll 1$ and noninteger $1/(1-\gamma^*)$.

It follows from this that in the vicinity of FS for $|\overline{p}|/\omega \cong 0$

$$\frac{\partial n(\overline{p})}{\partial \overline{p}} \sim \left(\frac{|\overline{p}|}{\omega}\right)^{-[(1-2\gamma^*)/(1-\gamma^*)]}. \tag{79}$$

Therefore if $1>2\gamma^*$ or $\gamma^*>1$ we have $\partial n(\overline{p})/\partial \overline{p} \rightarrow \infty$ when $\overline{p}/\omega \rightarrow 0$. In contrast for $\gamma^*<1$ and $1<2\gamma^*$ the momentum distribution function is a smooth function and there must be a charge gap in the regions of **k** space, where these conditions are satisfied. If we use our two-loop results we see that both sets of conditions are equally possible. Assuming that $\upsilon \ll \epsilon = \frac{2}{3}(\lambda-\Delta)$ we can use the value of U_x^* obtained before. Combining this with our perturbative result for $Z(\omega)$ which at the appropriate momentum value is given by

$$Z(\omega) = 1 - \frac{3}{32\pi^4 k_F^2}(\lambda-\Delta-\upsilon)^2 U_x^{*2} \ln\left(\frac{\Omega}{\omega}\right) + \cdots$$

$$\cong 1 - \frac{3}{32\pi^4 k_F^2}(\lambda-\Delta)^2 U_x^{*2} \ln\left(\frac{\Omega}{\omega}\right) \tag{80}$$

we find $\gamma^* \cong 6/121$. For this value of γ^* the momentum distribution function is clearly nonanalytic at $\overline{p}=0$ indicating that some remains of a Fermi surface continues to be present in the system. Thus for this **k**-space region the physical system resembles indeed a Luttinger liquid.[14,15] On the other hand if we choose our FS parameters in a way that $\gamma^* \cong 0.64$ we find that $\partial n(\overline{p})/\partial \overline{p} \rightarrow 0$ when $\overline{p}/\omega \rightarrow 0$ and the smoothness of $n(\overline{p})$ eliminates locally all traces of metallic behavior. As a result there should appear a charge gap along this direction of **k** space characterizing an associated insulating state. That a truncation of the Fermi surface could be produced by interaction was proposed earlier by Furukawa, Rice, and Salmhofer in the context of a $2d$-Hubbard model. Our result shows similar trends if certain condition concerning the Fermi surface parameters and the coupling fixed point are satisfied. This result is very suggestive in view of the fact that in high-T_c superconductors the Fermi surface has flat sectors and a pseudogap along preferential directions of momenta space.

This shows that the effects produced by the flat sectors of the FS leads to a complete breakdown of the Landau quasiparticle picture in the "cold" spots. This is in general agreement with recent photoemission data[6] for optimally doped Bi2212 which report a marginal Fermi liquid behavior for ImΣ and a large broadening of the spectral peak even around the $(\pi/2,\pi/2)$ region of the Fermi surface for temperatures higher than T_c. We find corrections for that marginal Fermi liquid behavior in our results. However, if the Fermi surface parameters in the metallic region are such that $\gamma^* \ll 1$ those corrections are logarithmically small and may not be easily detectable experimentally.

As we saw in our discussions so far our results depend in an important way on the value of the nontrivial fixed points. It is therefore opportune to check what happens to our results if we include higher-order corrections. To estimate them next we discuss the higher-loop contributions to both $\Sigma_\uparrow$ and $\Gamma^{(4)}_{\uparrow\downarrow;\uparrow\downarrow}$.

VI. HIGHER-ORDER CORRECTIONS

At three-loop order with our local subtraction regularization method we only do not distinguish the different bare coupling functions at the same order $O(U_0^3)$. There are in this way two contributions to the bare self-energy $\Sigma_{0\uparrow}$ (Fig. 4):

$$\Sigma_{0\uparrow}^{(a)}(p) = U_{0x}^3 \int_q G_\downarrow^{(0)}(q)[\chi_{\uparrow\downarrow}^{(0)}(q-p)]^2$$

$$= U_0^3 \int_q G_\downarrow^{(0)}(q)[\chi_{\uparrow\downarrow}^{(0)}(q-p)]^2 \tag{81}$$

and

$$\Sigma_{0\uparrow}^{(b)}(p) = U_{0C}^3 \int_q G_\downarrow^{(0)}(q)[\Pi_{\uparrow\downarrow}^{(0)}(q-p)]^2$$

$$= U_0^3 \int_q G_\downarrow^{(0)}(q)[\Pi_{\uparrow\downarrow}^{(0)}(q-p)]^2 \tag{82}$$

with $U_{0C}^3 \cong U_{0x}^3 \cong U_0^3$. There are four inequivalent ways of producing $\ln^2(\Omega/\omega)$ singularities with the Cooper blocks. In contrast there is only one exchange diagram at this order with the same kind of singularity. Since for $\mathbf{p}=(\Delta, -k_F+\Delta^2/2k_F)$ we have that $\Pi^{(0)}(\mathbf{q}+\mathbf{p};q_0+p_0) = -\chi_{\uparrow\downarrow}^{(0)}[\mathbf{q}-\mathbf{p};q_0-(-p_0)]$ the exchange channel diagram cancels one of the contributions from the Cooper channel and we end up with three Cooper $\ln^2(\Omega/\omega)$ singularities for $p_0=\omega\cong 0$. The next nonzero contributions are produced by the fourth-order terms shown in (Fig. 5). They all have the same relative sign bringing about a strong mix between the different scattering channels.

The calculation of all those higher order diagrams is highly nontrivial and is presently beyond the scope of this work. However, if we were to include such contributions we would automatically be forced to distinguish the different bare couplings already at two-loop order. This produces important changes in our earlier results. To observe this in detail we begin by rewriting our two-loop result for the quasiparticle weight $Z(\tilde{\mathbf{p}},\omega)$, for $\tilde{\mathbf{p}}=(\Delta,-k_F+\Delta^2/2k_F)$, as

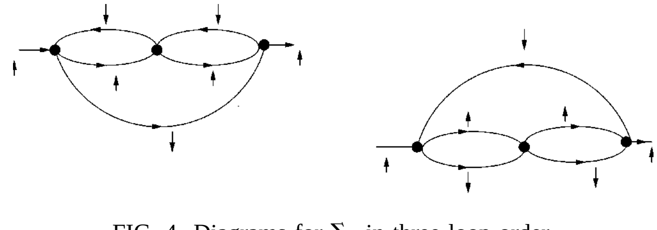

FIG. 4. Diagrams for $\Sigma_\uparrow$ in three-loop order.

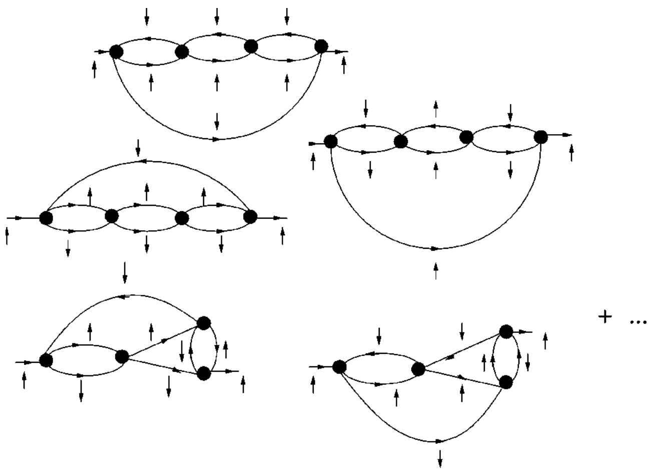

FIG. 5. Four-loop diagrams for $\Sigma_{\uparrow}$.

$$Z^{-1}(\tilde{\mathbf{p}},\omega)=1+\frac{3}{64\pi^4 k_F^2}(\lambda-\Delta)^2\ln\left(\frac{\Omega}{\omega}\right)(U_{0x}^2+U_{0C}^2)+\cdots \tag{83}$$

and for $Z(\mathbf{p}^*,\omega)$ at $\mathbf{p}^*=(\lambda-\epsilon,-k_F+\Delta^2/2k_F)$:

$$Z(\mathbf{p}^*,\omega)=1+\frac{3}{32\pi^4 k_F^2}[(\lambda-\Delta)^2+2\epsilon(\lambda-\Delta-\epsilon)]\ln\left(\frac{\Omega}{\omega}\right)\times(U_{0x}^2+U_{0C}^2)+\cdots. \tag{84}$$

The numerical difference between these two Z values is essentially due to the longitudinal components of $\tilde{\mathbf{p}}$ and $\mathbf{p}^*$, respectively.

If we repeat the same procedure as before but now distinguishing the diverse bare coupling functions at two-loop order we find, respectively,

$$U_x(\mathbf{p}_1-\mathbf{p}_4;\omega)=U_{0x}+\left[\frac{\epsilon}{2\pi^2 k_F}U_{0x}^2-bU_{0x}(U_{0x}^2+U_{0C}^2)-\frac{(\lambda-\Delta-\epsilon)}{2\pi^2 k_F}U_{0C}^2\right]\ln\left(\frac{\Omega}{\omega}\right)+\cdots, \tag{85}$$

$$U_f(\mathbf{p}_1-\mathbf{p}_3;\omega)=U_{0f}-\left[\frac{(\lambda-\Delta-\epsilon)}{2\pi^2 k_F}U_{0C}^2+bU_{0f}\times(U_{0x}^2+U_{0C}^2)\right]\ln\left(\frac{\Omega}{\omega}\right)+\cdots, \tag{86}$$

$$U_C(\mathbf{p}_1=-\mathbf{p}_2;\omega)=U_{0C}-\left[\frac{4\lambda}{2\pi^2 k_F}U_{0C}^2+bU_{0x}(U_{0x}^2+U_{0C}^2)-\frac{(\lambda-\Delta-\epsilon)}{4\pi^2 k_F}U_{0x}^2\right]\ln\left(\frac{\Omega}{\omega}\right). \tag{87}$$

for the exchange, forward, and Cooper channels. If we now define the corresponding β functions as

$$\beta_x(U_x,U_f,U_C)=\omega\frac{\partial U_x}{\partial\omega}, \tag{88}$$

$$\beta_f(U_f,U_x,U_C)=\omega\frac{\partial U_f}{\partial\omega}, \tag{89}$$

$$\beta_C(U_C,U_x,U_f)=\omega\frac{\partial U_C}{\partial\omega} \tag{90}$$

it follows that

$$\beta_x(U_x,U_f,U_C)=-\frac{\epsilon}{2\pi^2 k_F}U_x^2+bU_x(U_x^2+U_C^2)+\frac{(\lambda-\Delta-\epsilon)}{2\pi^2 k_F}U_C^2+\cdots, \tag{91}$$

$$\beta_f(U_f,U_x,U_C)=\frac{(\lambda-\Delta-\epsilon)}{2\pi^2 k_F}U_C^2+bU_f(U_x^2+U_C^2)+\cdots \tag{92}$$

and

$$\beta_C(U_C,U_x,U_f)=\frac{4\lambda}{2\pi^2 k_F}U_C^2+bU_C(U_x^2+U_C^2)-\frac{(\lambda-\Delta-\epsilon)}{4\pi^2 k_F}U_x^2+\cdots \tag{93}$$

with b given as before. To determine the fixed points we have to solve these coupled equations. As we emphasized before the fixed point values vary as we move along the Fermi surface. This reflects the explicit role played by the momenta components projected along the FS.

In order to illustrate what might happen to the fixed points in the presence of mixing of scattering channels let us choose for simplicity the case $\epsilon=\lambda-\Delta$. Taking $\beta_x=\beta_f=\beta_C=0$ it follows immediately that the non-trivial fixed points for this value of ϵ are

$$U_x^*=\frac{16\pi^2 k_F}{3(\lambda-\Delta)}\zeta^{-1}, \tag{94}$$

$$U_f^*=0, \tag{95}$$

$$U_C^*=-\frac{4\pi^2 k_F}{3\lambda}\zeta^{-1} \tag{96}$$

with $\zeta=\{1+[(\lambda-\Delta)/4\lambda]^2\}>1$. Defining the matrix of eigenvalues M_{ij} by

$$M_{ij}=\left(\frac{\partial\beta_i}{\partial U_j}\right)_{U^*} \tag{97}$$

for $i,j=C,x,f$ respectively we can expand in coupling space around these fixed points to find[16,17]

$$\beta_i\cong\sum_j M_{ij}[U_j(\mathbf{p}^*;\omega)-U_j^*(\mathbf{p}^*)]+\cdots. \tag{98}$$

Integrating these out we obtain

$$U_i = U_i^* + \sum_j c_j V_j^i \omega^{\gamma_j}, \tag{99}$$

where

$$M_{ij} V_{ij} = \gamma_i V_i . \tag{100}$$

Using our results it then turns out that

$$U_C(\mathbf{p}^*;\omega) \cong U_C^* - \frac{c_1}{\sqrt{2\zeta}} \left(\frac{\lambda - \Delta}{4\lambda} \right) \omega^{(8/3)\zeta^{-1}} + \frac{c_2}{\sqrt{\zeta}} \omega^{-(8/3)\zeta^{-1}}, \tag{101}$$

$$U_x(\mathbf{p}^*;\omega) \cong U_x^* + \frac{c_1}{\sqrt{2\zeta}} \omega^{(8/3)\zeta^{-1}} + \frac{c_2}{\sqrt{\zeta}} \left(\frac{\lambda - \Delta}{4\lambda} \right) \omega^{-(8/3)\zeta^{-1}}, \tag{102}$$

and

$$U_f(\mathbf{p}^*;\omega) \cong \frac{c_1}{\sqrt{2}} \omega^{(8/3)\zeta^{-1}}, \tag{103}$$

where c_1, and c_2 are constants. As a result unless there is a new adjustable parameter which would be tunned to produce $c_2 = 0$ the fixed point (U_C^*, U_x^*, U_f^*) is infrared unstable when we approach the Fermi surface by taking the limit $\omega \rightarrow 0$. This is the main effect produced by the mixing of scattering channels at higher order perturbation theory at this sector of the FS. This is again an interesting result in view of the fact that the pseudogap state in the underdoped cuprates does not seem to be a realizable state at $T = 0$. It would therefore be natural to associate such a phase in the cuprates to an unstable fixed point.

Since the running coupling functions $U_C(\mathbf{p};\omega)$ and $U(\mathbf{p};\omega)$ are only infrared stable if there exists an external parameter which could either be, e.g., temperature or hole concentration, it can be readily adjusted to nullify c_2 at the FS. The critical surface formed by the set of trajectories of $U_i(\mathbf{p}^*;\omega)$ which are attracted into the fixed point (U_C^*, U_x^*, U_f^*) for $\omega \rightarrow 0$, in this case, has in this way codimensionality one. If we represent such external parameter needed by θ, it turns out that in the vicinity of the phase transition the coupling constants associated with the three scattering channels become

$$U_C(\omega) \cong U_C^* + - \frac{c_1}{\sqrt{2\zeta}} \left(\frac{\lambda - \Delta}{4\lambda} \right) \omega^{(8/3)\zeta^{-1}} + \frac{(\theta - \theta_c)}{\sqrt{\zeta}} \omega^{-(8/3)\zeta^{-1}}, \tag{104}$$

$$U_x(\omega) \cong U_x^* + \frac{c_1}{\sqrt{2\zeta}} \omega^{(8/3)\zeta^{-1}} + \frac{(\theta - \theta_c)}{\sqrt{\zeta}} \left(\frac{\lambda - \Delta}{4\lambda} \right) \omega^{-(8/3)\zeta^{-1}}, \tag{105}$$

and

$$U_f(\omega) \cong \frac{c_1}{\sqrt{2}} \omega^{(8/3)\zeta^{-1}}, \tag{106}$$

where θ_c is the critical value of θ at the transition point.

VII. CONCLUSION

We present a two-loop field-theoretical renormalization group calculation of a two-dimensional truncated Fermi surface. Our Fermi surface model consists of four disconnected patches with both flat pieces and conventionally curved arcs centered around $(0, \pm k_F)$ and $(\pm k_F, 0)$ in $\mathbf{k}$ space. Two-dimensional Fermi-liquid-like states are defined around the central region of each patch. In contrast the patch border regions are flat and as a result their associated single particle states have linear dispersion law. These flat sectors are introduced specifically to produce nesting effects which in turn generate logarithmic singularities in the particle-hole channels which are known to induce non-Fermi-liquid effects. In this way conventional $2d$ Fermi-liquid states are sandwiched by single particles with a linear dispersion law to simulate the so-called "cold" spots as in the experimentally observed truncated Fermi surface of the underdoped normal phase of the high-temperature superconductors. Our main motivation here is to test to what extent Fermi-liquid theory is applicable in the presence of flat Fermi surface sectors which are indicative of a strong coupling regime. New experimental data on both optimally doped and underdoped Bi2212 (Ref. 6) above T_c indicate that the imaginary part of the self-energy $\mathrm{Im}\,\Sigma(\omega)$ scales linearly with ω even along the (0,0)-(π,π) direction. This is consistent with other photoemission experiments[6] which support a marginal Fermi-liquid phenomenology over the whole Fermi surface. Our results are in general agreement with those experimental findings since the power law corrections we find for this linear behavior can in some cases be so small as not to be detectable by the present day experiments. Using perturbation theory we calculate the two-loop self-energy of a single particle associated with a curved FS sector. We find that the bare self-energy is such that $\mathrm{Im}\,\Sigma_0(\omega) \sim \omega$ and as a result $\mathrm{Re}\,\Sigma_0(\omega) \sim \omega \ln(\Omega/\omega)$ for $\omega \sim 0$ reproducing the marginal Fermi-liquid phenomenology at the FS. We calculate Σ_0 as a function of both frequency and momentum. It turns out that both $\partial \Sigma_0 / \partial p_0$ and $\partial \Sigma_0 / \partial \overline{p}$ diverge at the FS. Using RG theory we determine the renormalized one-particle irreducible function $\Gamma_R^{(2)}(p_0, \mathbf{p}; U, \omega)$ in the vicinity of a "cold" spot FS point. Again it follows immediately that the quasiparticle weight Z vanishes identically at the Fermi surface. Next we calculate the bare one-particle irreducible two-particle function $\Gamma_{0\alpha\beta}^{(4)}(p_1, p_2; p_3, p_4)$ for $\alpha, \beta = \uparrow, \downarrow$. This function depends on the spin arrangements as well as on the relative momenta of its external legs. There are three different scattering channels associated with the $\Gamma_{0\alpha\beta}^{(4)}$'s: the so-called Cooper, exchange, and forward channels. For a FS with flat sectors there are logarithmic singularities in $\Gamma_{0\alpha\beta}^{(4)}$

for both exchange and forward channels due to nesting effects. In contrast the Cooper channel produces similar singularities in the whole FS. We calculate $\Gamma_0^{(4)}$ perturbatively up to two-loop order for the mentioned scattering channels. Taking into account self-energy corrections calculated earlier on we obtain the corresponding renormalized one-particle irreducible function $\Gamma_R^{(4)}$ subjected to an appropriate renormalization condition. The field theory regularization scheme allows us to introduce local counterterms to cancels all divergences order by order in perturbation theory. This simplifies the problem considerably although due to the anisotropy in **k** space the counterterms are in fact momenta dependent. The bare coupling constant becomes a bare coupling function and we proceed with the regularization of the divergences grouping them together according to their location at the FS, the scattering channel, and the vertex type interaction. We introduce in this way three bare coupling functions $U_{0x}(\mathbf{p})$, $U_{0C}(\mathbf{p})$, and $U_{0f}(\mathbf{p})$ to systematically cancel all the local divergences in our perturbation theory expansions. In this scheme the effects produced by the crossing of different channels is practically nonexistent up to the two-loop order calculation of the self-energy. Therefore if we only consider the leading divergence at every order of perturbation theory it is essential to proceed with the renormalization of fields in order for the running coupling functions to develop nontrivial infrared (IR) stable fixed points. As opposed to the parquet or the Wilsonian RG methods we do not try to derive an effective action in explicit form. This would in practice demand the introduction of an infinite number of local counterterms in our Lagrangian model. Nevertheless all divergences can be removed to all orders by local subtractions around a given point of momentum space. The anisotropy of the Fermi surface therefore reflects itself directly in the momentum dependence of the coupling parameters. This feature is consistent with the findings of those other two approaches referred to before. Since we take explicitly into account self-energy effects we are able to find nontrivial fixed point solutions even if we do not go beyond the leading divergence approximation in our higher loop calculations. With our two-loop results for the nontrivial fixed points together with the assumption that the physical system acquires a critical condition as we approach the Fermi surface, by taking the scale parameter $\omega \to 0$, we can solve the RG equation for the renormalized single particle propagator $G_R(p;U,\omega)$ in the vicinity of a chosen "cold" spot point. We show that the nullification of the quasiparticle weight Z manifests itself as an anomalous dimension in G_R. This anomalous dimension is independent of the sign of the given fixed point value. Using this result we calculate the spectral function $A_R(p;U^*,\omega)$ and the renormalized single particle dispersion law. From this we calculate the "Fermi velocity" which can either remain finite or is nullified at the FS. Finally we calculate the corresponding momentum distribution function $n(\overline{p})$ in the vicinity of the FS and show that it is a continuous function of $\overline{p}$ with $\partial n(\overline{p})/\partial \overline{p}$ finite or $\partial n(\overline{p})/\partial \overline{p} \to \infty$ when $\overline{p}/\omega \to 0$. In the former case we have a real charge gap typical of an insulating state and in the latter the physical system continues to be metallic and resembles a Luttinger liquid. There could be in this way phase separation in **k** space and there is a complete breakdown of the Landau Fermi liquid when the "cold" spot suffers the effects produced by the flat FS sectors. Since essentially the RG exponentiates the self-energy ln corrections the power law behavior of G_R reflects itself back in the renormalized self-energy producing

$$\mathrm{Im}\,\Sigma_R(\mathbf{p};U^*) \sim -|p_0| \left(\frac{p_0^2}{\omega^2} \right)^{-\gamma^*(\mathbf{p};U^*)/2} \tag{107}$$

with γ^* depending on the size of the size of the flat Fermi surface sectors through the fixed point coupling strength. For certain **k**-space regions near the FS we show that $\gamma^* \simeq 6/121$. This produces a singular $\partial n(\overline{p})/\partial \overline{p} \to \infty$ and is consistent with the marginal Fermi liquid phenomenology which is in agreement with the observed experimental results which are not sensitive enough to distinguish such minor power law corrections.

Since several of our results are given in terms of a fixed point value it is important to see what happens if we consider higher order contributions to our perturbation theory expansions. We do this calculating initially the three-loop corrections to the bare self-energy $\Sigma_{0\uparrow}$. At this order of perturbation theory we have the bare constants $U_{0C}^3 \cong U_{0x}^3 \cong U_{0f}^3$ identical to each other. However, if we consider higher order terms in our perturbative calculation of the three bare couplings we can distinguish the different contributions produced at order $O(U_0^2)$ and this brings important changes to our results. The exchange and Cooper channel couplings mix strongly with each other. As a result of this we define generalized β functions $\beta_i = \omega \partial U_i / \partial \omega = \beta_i(U_C, U_x, U_f)$ for $i = C,x,f$. We calculate the eigenvalue matrix $M_{ij} = \partial \beta_i / \partial U_j^*$, find its eigenvalues, and expand these β functions in coupling space around one of the existing fixed points in **k** space. We then show that the critical surface formed by the set of trajectories of $U_i(\mathbf{p};\omega)$ which is attracted into the fixed point $[U_C^*(\mathbf{p}), U_x^*(\mathbf{p}), U_f^*(\mathbf{p})]$ for $\omega \to 0$ has codimensionality one. This means that the fixed point is infrared unstable and one external parameter is needed to drive the physical system towards one of its stable phases. This result is very suggestive since the underdoped phase of the cuprates at finite temperature is well characterized by a pseudogap state. This state may not be realizable at zero temperature and may also well be associated with such an unstable fixed point.

To conclude it is fair to say that even a simplified anisotropic Fermi surface model such as the one used in this work is able to produce interesting nontrivial results due to the fact that it contains flat parts which are indicative of a strong interaction regime. They turn the $2d$-Fermi-liquid states into a non-Fermi liquid which can be metallic or insulating depending on its location at the Fermi surface in **k** space. It is tempting to relate our results to the high-T_c superconductors which are also known to have an anisotropic FS displaying non-Fermi-liquid behavior for both the underdoped and optimally doped metallic phase, above the critical temperature. The underdoped cuprates are also notorious for presenting a pseudogap state at finite temperature. Our findings concerning the nature of the metallic state are in general agreement with more recent photoemission experiments which demonstrate the validity of the marginal Fermi liquid phenomenology above T_c. We believe therefore that the model presented here might well contain some of the ingredients which are needed to describe the strange metal and the pseudogap phases of the cuprate superconductors.

ACKNOWLEDGMENTS

I am grateful to T.M. Rice, C. Honerkamp, and K. Voelker (ETH–Zurich) and D. Baeriswyl, B. Binz, C. Morais-Smith, and C. Aebischer (ITP–Fribourg) for several stimulating discussions. Discussions with Peter Kopietz and with Benham Farid are also greatly appreciated. Finally I also want to thank the Center for Theoretical Studies-ETH-Zurich, the Institute de Physique Theorique–University de Fribourg and the Swiss National Foundation for their very nice hospitality. This work is partially supported by the CNPq (Brazil).

*Permanent address: Centro Intl. de Fis. da Mat. Condensada-UnB, Brasilia-DF (Brazil).

[1] J.R. Schrieffer, X.G. Wen, and S.C. Zhang, Phys. Rev. B **39**, 11 663 (1989); Y.M. Vilk, L. Chen, and A.M.S. Tremblay, **4**, 13 267 (1994); T. Saikawa and A. Ferraz, Eur. Phys. J. B **20**, 65 (2001).

[2] See, e.g., N. Furukawa, T.M. Rice, and M. Salmhofer, Phys. Rev. Lett. **81**, 3195 (1998); J. Gonzalez, F. Guinea, and M.A.H. Vozmediano, *ibid.* **79**, 3514 (1997); Nucl. Phys. B 485 694; J. Gonzalez, Phys. Rev. B **63**, 045114 (2001); H.J. Schulz, Europhys. Lett. **4**, 609 (1987); I.E. Dzyaloshinskii, Sov. Phys. JETP **66**, 848 (1987); J. Ruvalds *et al.* Phys. Rev. B **51**, 3797 (1995).

[3] A. Luther, Phys. Rev. B **50**, 11 446 (1994).

[4] J.C. Campuzano *et al.* Phys. Rev. Lett. **64**, 2308 (1990); D.S. Dessau *et al. ibid.* **71**, 2781 (1993); A.G. Loeser *et al.* Science **285**, 325 (1996); H. Ding *et al.* Nature (London) **382**, 51 (1996).

[5] R. Hlubina and T.M. Rice, Phys. Rev. B **51**, 9253 (1995); B.P. Stojkovic and D. Pines, Phys. Rev. Lett. **76**, 811 (1996).

[6] T. Valla *et al.* Science **273**, 2110 (1999); Phys. Rev. Lett. **85**, 828 (2000); A. Kaminski *et al.*, *ibid.* **84**, 1788 (2000); cond-mat/0004482 (unpublished); P.V. Bogdanov *et al.*, Phys. Rev. Lett. **85**, 2581 (2000).

[7] A. Ferraz, T. Saikawa, and Z.Y. Weng, Mod. Phys. Lett. B **3**, 1031 (1999).

[8] A.T. Zheleznyak, V.M. Yakovenko, and I.E. Dzyaloshinskii, Phys. Rev. B **55**, 3200 (1998).

[9] D. Zanchi and H.J. Schulz, Phys. Rev. B **61**, 13 609 (2000); C.J. Halboth and W. Metzner, *ibid.* **61**, 7364 (2000); C. Honerkamp *et al.*, *ibid.* **63**, 035109 (2001); P. Kopietz and T. Busche, *ibid.* **64**, 155101 (2001); T. Busche *et al.* J. Phys.: Condens. Matter **14**, 8513 (2002); B. Binz, D. Baeriswyl, and B. Ducot, Eur. Phys. J. B **25**, 69 (2002).

[10] R. Shankar, Rev. Mod. Phys. **66**, 129 (1994); J. Polchinski, in *1992 TASI in Elementary Particle Physics*, edited by J.Harvey and J. Polchinski (World Scientific, Singapore, 1992).

[11] A. Ferraz, Mod. Phys. Lett. B **17**, 167 (2003).

[12] C.M. Varma *et al.* Phys. Rev. Lett. **63**, 1996 (1989).

[13] See, e.g., J.C. Collins, *Renormalization* (Cambridge University Press, Cambridge, 1985); S. Pokorski, *Gauge Field Theories* (Cambridge University Press, Cambridge, 1987).

[14] D.C. Mattis and E.H. Lieb, J. Math. Phys. **6**, 304 (1965).

[15] P.W.Anderson, *The Theory of Superconductivity in High T_c Cuprates* (Princeton University Press, Princeton, 1997); see also B. Farid, Philos. Mag. B **79**, 1097 (1999).

[16] See, e.g., S. Weinberg, *The Quantum Theory of Fields* (Cambridge University Press, Cambridge, 1996).

[17] J. Solyom, Adv. Phys. **28**, 201 (1979).